Available online at www.sciencedirect.com
SCIENCE DIRECT®

Journal of the European Ceramic Society 26 (2006) 1561–1565

www.elsevier.com/locate/jeurceramsoc

Formation of micron-sized and nanometer-sized single crystal alumina whiskers by displacement reactions

Dickon H.L. Ng[a,*], P. Yu[a], N.G. Ma[a], C.K. Lo[a], W.Y. Kwok[a], M.Y. Yau[a], C.Y. To[a], T.K. Li[a], Cheng-Ji Deng[b]

[a] *Department of Physics, The Chinese University of Hong Kong, Shatin, Hong Kong, China*
[b] *Hubei Province Key Laboratory of Ceramics and Refractories, Wuhan University of Science and Technology, Wuhan, China*

Received 19 January 2005; received in revised form 24 February 2005; accepted 5 March 2005
Available online 8 April 2005

Abstract

We propose a general methodology for fabricating single crystal α-Al_2O_3 whiskers by displacement reactions. The methodology is based on studies in which Al-rich powder mixtures that contain different kinds of metal oxides (MO_x) were sintered. In some sintered products, the in situ formed Al_2O_3 appeared as particulate while in other it appeared as whiskers. Some conclusions from this study are: growth of the whiskers involves the presence of MO_{x-1} vapor and Al_2O vapor during sintering, and the dimension of the whiskers depends on the size of the initial MO_x particles. Micron-sized whiskers were produced in Al–MoO_3 and in Al–WO_3, while nanorods were produced in Al–SiO_2.

Keywords: Al_2O_3; SiO_2; Sintering; Whiskers

1. Introduction

Alumina (Al_2O_3) is widely used in engineering applications as dielectric substrates, biomaterials,[1] automobile parts and optical devices.[2] The early fabrication of Al_2O_3 whiskers was reported by Webb et al.[3] Currently, the use of whiskers and fibers is found in optical devices,[2] and in composites in which Al_2O_3 usually acts as reinforcement.[4] Since the discovery of carbon nanotubes,[5] there are a large number of investigations on one-dimension (1D) nanometer-sized (nm-sized) structures such as nanorods and nanowires.[6–8] These products have included metal oxides such as MgO,[9] Ga_2O_3,[10] ZnO,[11] and SiO_2[12] that are synthesized by laser ablation,[13] template,[14] arc discharge,[15] or vapor-phase transport.[16] They have received a great deal of attention because of their remarkable properties and potential applications.[17,18] Currently, 1D nm-sized Al_2O_3 is commonly used as light emitting materials[19,20] and in catalyst devices.[21]

The micron-sized and nm-sized Al_2O_3 whiskers, like many 1D materials, are usually fabricated by complicated and costly methods involving high temperatures, such as the template method and the vapor–liquid–solid process (VLS).[22] The template method, in which polycrystalline Al_2O_3 nanotubes or single crystal nanowires are produced,[8] uses carbon nanotubes as templates. The VLS process requires molten liquid that acts as transfer medium for deposition from gaseous Al_2O_3.[6–8] Many of these methods involve the use of catalysts, thus their products often contain impurities. Recently, we successfully fabricated micron-sized and nm-sized single crystal α-Al_2O_3 whiskers by sintering a mixture of Al and MoO_3,[4] and a mixture of Al and SiO_2,[23] respectively. As an extension of these previous works, we now report studies of different Al–metal oxide (MO_x) systems. A general methodology for producing α-Al_2O_3 whiskers is established and the growth mechanism of the whiskers in these Al–MO_x systems is described.

* Corresponding author. Tel.: +852 2609 6392; fax: +852 2603 5204.
E-mail address: dng@phy.cuhk.edu.hk (D.H.L. Ng).

0955-2219/$ – see front matter
doi:10.1016/j.jeurceramsoc.2005.03.233

Table 1
The initial particle sizes of the metal oxides (MO_x), their mixing ratios with the Al powder, and their corresponding Al_2O_3 products after sintering

	Metal oxide (MO_x)					
	MoO_3	WO_3	SiO_2	NiO	ZnO	CuO
Size of raw powder (μm)	0.5–3	0.1–1	0.015	0.5–3	0.5–3	3–10
Al:MO_x ratio (in weight)	9:1	9:1	1:1	8:2	9:1	8:2
Size of Al_2O_3 product (μm)	Type of Al_2O_3 product					
	Whisker			Particle		
Width	1–1.5	0.2–0.5	0.05	1–3	5–10	3–5
Length	10	8	5–10			

2. Experiments

The samples were prepared from Al powder (99.8% purity and −325 mesh) and high purity (>99%) metal oxide (MO_x) powders ($MO_x = MoO_3$, WO_3, SiO_2, CuO, ZnO, or NiO). The initial particle sizes of the MO_x powders, and their mixing ratios with Al are listed in Table 1. The Al–MO_x was mixed and ground in a mortar for an hour before the powder mixture was pressed under 200–500 MPa to form 2 mm thick discs with diameter of 10 mm. The Al–MO_x disc was sintered at a temperature in the range between 805 and 1150 °C in Ar atmosphere for about 2 h before it was cooled down to room temperature inside the furnace with the power turned off. The phases in the sintered sample were determined by X-ray diffractometry (XRD). Microstructural and elemental analyses were conducted by scanning electron microscopy (SEM) and energy dispersive X-ray spectrometry (EDS), respectively. Some of the samples, prior to SEM examination, were etched by 1 M NaOH solution to remove the Al metal, so that the morphology of the in situ products could be revealed. For the investigation of whiskers by using transmission electron microscopy (TEM), whiskers were extracted by etching the sintered samples in 10% HF–10% HNO_3 solution (for removing the Al–M intermetallics). Residual precipitates containing the corrosion-resistant whiskers were rinsed with water and ethanol before the TEM examination.

3. Results and discussion

Fig. 1 shows the XRD patterns of some of the sintered Al–MO_x products ($MO_x = SiO_2$, MoO_3, CuO, and NiO). In these samples, peaks that correspond to Al, Al_2O_3, Al–M intermetallics (e.g. Al_2Cu, Al_3Mo, Al_3Ni) are found, while no peak corresponding to intermetallic phase is found in the XRD pattern of the Al–SiO_2 sample. These results indicate that one or more reactions had occurred during sintering, in which MO_x was reduced to M, and Al was oxidized to Al_2O_3. Based on the SEM images of the sintered samples, the products can be divided into two groups: one contains whiskers and the other does not. Fig. 2a–c show the microstructures of the first group of Al–MO_x products where

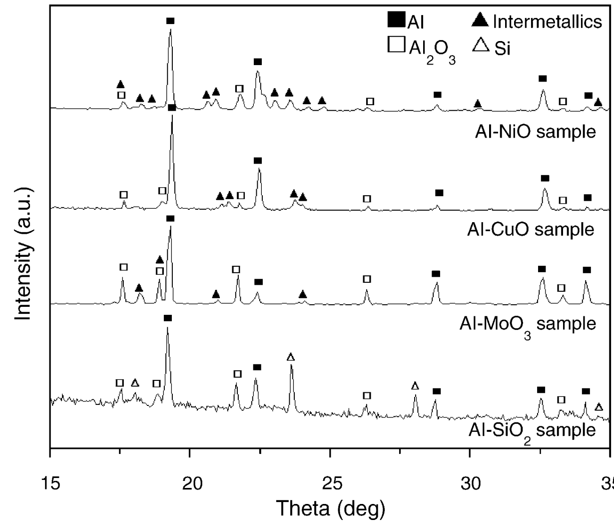

Fig. 1. XRD diffraction patterns of some of the sintered Al–MO products.

MO_x is MoO_3, WO_3, or SiO_2. In these samples, a large number of whiskers are found in the matrices of the sintered samples. These whiskers emerged isotropically from the matrix grains. The size of the whiskers in the sintered Al–MoO_3 (Fig. 2a) appears larger than that in the sintered Al–WO_3 (Fig. 2b). The former has a width of ∼1–1.5 μm and ∼10 μm in length, while the latter has a width of ∼0.2–0.5 μm and length of ∼8 μm. As for the sintered Al–SiO_2 (Fig. 2c), the whiskers are typically ∼5–10 μm long, while their diameter is in the nanometer range and can only be resolved accurately by TEM. Fig. 2d–f show the micrographs of the second group of Al–MO_x (i.e. $x = 1$) sintered products with MO_x equal to CuO, NiO or ZnO, in which Al_2O_3 appears in the form of particulate. The particulate ranges from 1 to 10 μm in size. In the Al–CuO system, MO_x was reduced to Cu and followed by formation of Al–Cu. A two-phase Al–Al_2Cu eutectic was produced when molten Al–Cu solidified. Similar events also occurred in the Al–NiO system. For Al–ZnO, after the reduction of ZnO, Zn sublimed and left Al_2O_3 particulate in the Al matrix of the sample.

Extracted whiskers from the sintered samples (group shown in Fig. 2a–c) were more closely investigated. The whiskers from the Al–MoO_3 sample were studied by SEM. Fig. 3a is a SEM micrograph that shows one of these whiskers with size of ∼1.5 μm. The EDS analysis taken from this whisker shows that the atomic ratio of Al to O is 39–61, and proves that it is Al_2O_3. The whiskers from the Al–WO_3 and Al–SiO_2 were investigated by TEM, their images are shown in Fig. 3b and c, respectively. The one extracted from Al–WO_3 is about ∼0.5 μm thick and that from Al–SiO_2 is ∼50 nm. Selected area electron diffraction (SAED) was conducted near the tips of these two whiskers. Their SAED patterns are shown in the insets of their micrographs. It is found that the corresponding pattern of each whisker belongs to a single crystal hexagonal alpha phase Al_2O_3, thus confirms that the whisker is single crystal α-Al_2O_3.

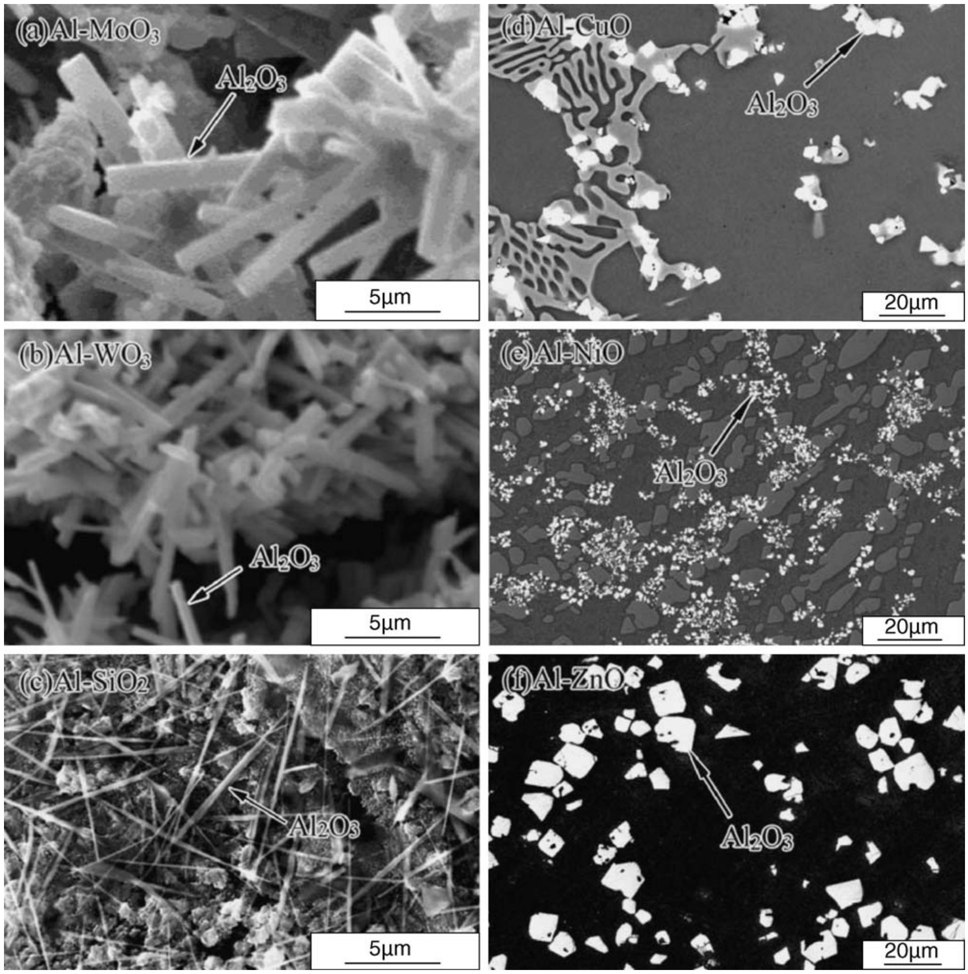

Fig. 2. (a)–(c) SEM images of the sintered samples which contain in situ formed α-Al_2O_3 whiskers. (d)–(f) SEM images of the sintered samples contain in situ formed particulate.

4. Whiskers formation

The growth of whisker from its tip can be described by the vapor–liquid–solid (VLS) mechanism[24,25] or the vapor–solid (VS) mechanism.[26] In the VLS process, the growth is initiated by condensation of vapor of the material onto a catalyst at the tip of the whisker, whereas the VS process involves condensation of vapor onto screw dislocations and the vapor is directly converted into solid. The VLS mechanism is widely adopted to describe the growth of 1D Al_2O_3 nanowires,[6] nanobelts,[7] or nanotrees.[8] In many cases, metal impurity is being used as catalyst, having relatively lower melting point. It acts as a preferred site for deposition from gaseous Al_2O_3. As the droplet becomes supersaturated with Al_2O_3, the whisker grows by precipitating Al_2O_3 from the molten metal. An example of growing Al_2O_3 whisker by VLS process was the work performed by Kim et al.[27] in which basal sapphire and molten Pt were used as substrate and catalyst, respectively. A strong evidence for the VLS growth in these products is based on the morphology of their whiskers in which round droplets are usually found near their tips.[20,28] In our work, we observed that the tips of the micron-sized or the nm-sized α-Al_2O_3 whiskers in our sintered products (after slightly etched and intensively etched) were typically round or slightly sharp, and no droplet-tips were found (Fig. 3). This observation suggests that the growth of whiskers in this work follows another route.

The Ostwald ripening mechanism[29,30] describes particle growth by coarsening that involves mass transfer of a two-phase mixture driven by the reduction of interfacial energy. This may be a probable explanation to unlock the growing process of α-Al_2O_3 whiskers in our sintered Al–MO_x products (where $x = 2$ or 3). With reference to the works by Brewer and Searcy,[31] and by Sosman,[32] the possible reactions in the Al–MO_x system during sintering were:

$$2x\mathrm{Al}_{(l)} + 3\mathrm{MO}_{x(s)} \rightarrow x\mathrm{Al_2O}_{3(s)} + 3\mathrm{M}_{(s,l)} \quad (1)$$

$$\mathrm{M}_{(l)} + (x-1)\mathrm{MO}_{x(s)} \rightarrow x\mathrm{MO}_{x-1(g)} \quad (2)$$

$$4\mathrm{Al}_{(l)} + \mathrm{Al_2O}_{3(s)} \rightarrow 3\mathrm{Al_2O}_{(g)} \quad (3)$$

$$(x-1)\mathrm{Al_2O}_{(g)} + 2\mathrm{MO}_{x-1(g)} \rightarrow (x-1)\mathrm{Al_2O}_{3(s)} + 2\mathrm{M}_{(s,l)} \quad (x = 2, 3) \quad (4)$$

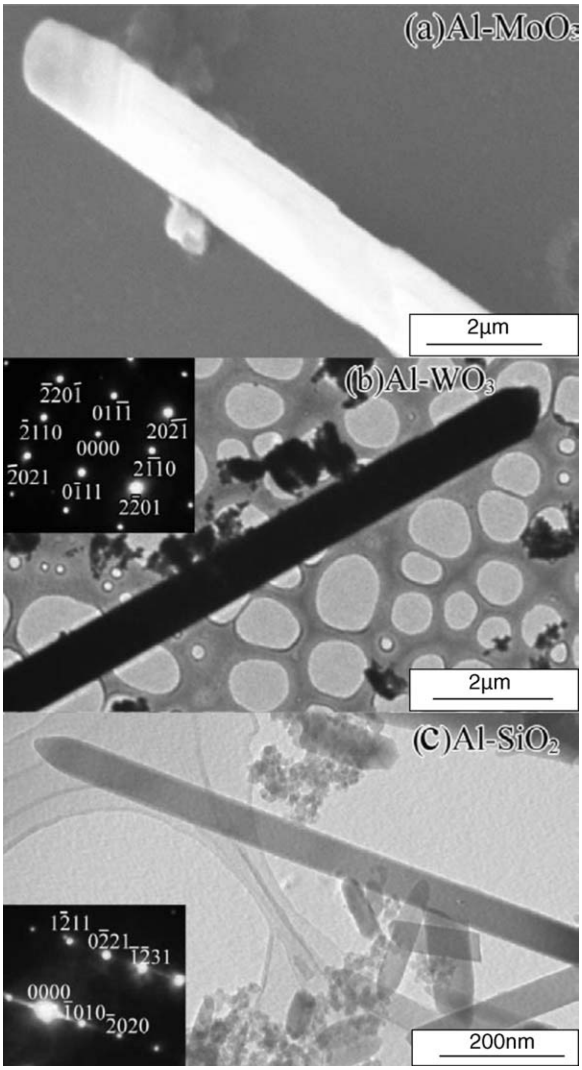

Fig. 3. Top micrograph is a SEM image of an α-Al_2O_3 whisker extracted from the Al–MoO_3 sintered sample. Middle and bottom micrographs are the TEM images and their corresponding SAED patterns of α-Al_2O_3 whiskers extracted from the Al–WO_3 and Al–SiO_2 sintered samples, respectively.

where subscripts s, l, and g represent whether the reactant or the product was in the form of solid, liquid or gas phase, respectively. As the sintering temperature reached 660 °C, Al started to melt. The displacement reaction (Eq. (1)) occurred at points where MO_x (MoO_3, WO_3, or SiO_2) and molten Al made contact to produce metal M and the precursor Al_2O_3. The size of the precursor was possibly smaller than (if not equal to) the size of the raw MO_x particle. When the newly formed M (i.e. Mo, W, or Si) entered the molten Al, the viscosity of the melt decreased. Consequently, the liquid mixture provided favorable fluidity for nucleation and crystallization of whiskers.[30] When MO_x and Al_2O_3 were further in contact with the molten Al–M mix, MO_{x-1} (i.e. MoO_2, WO_2 or SiO) and Al_2O in vapor phases were produced (Eqs. (2) and (3)), respectively. When MO_{x-1} and Al_2O vapors reacted, Al_2O_3 was produced (Eq. (4)). These small Al_2O_3 particles then coarsened onto the larger Al_2O_3 precursors in the ripening process. It is known that surface energies (γ) of different crystallographic planes are usually different. In hexagonal alumina crystal, the surface energies are $\gamma(0\,0\,1) > \gamma(1\,0\,0) > \gamma(10\bar{2})$.[33] Thus, the driving force for coarsening would be more intense in the (0 0 1) plane, and the alumina particles would tend to join the growing rod at the tip where the (0 0 1) plane was. As a result, the alumina rods grew toward the [0 0 1] direction in ripening.

As mentioned, the size of the precursors is related to the size of the raw MO_x particles. Our SEM work reveals that the average sizes of the raw MoO_3 and WO_3 particles are ~0.5–3 μm and ~0.1–1 μm, respectively, as shown in Fig. 4. Therefore, it is reasonable to postulate that the Al_2O_3 precursors in Al–MoO_3 and Al–WO_3 are micron-sized, and that the diameters of the full-grown whiskers in these two systems are also micron-sized. Such a claim is confirmed by the facts that (i) micron-sized α-Al_2O_3 whiskers were found in the Al–MoO_3 and Al–WO_3 systems, (ii) the whiskers in Al–MoO_3 were thicker than those of the Al–WO_3, and (iii) nm-sized whiskers were found in Al–SiO_2 where the starting SiO_2 powder had a particle size of ~15 nm. The size of the MO_x raw powders and their corresponding Al_2O_3 products are summarized in Table 1.

Some other facts have also emerged from this study. There must be a rich supply of molten Al and metal M as nutrients for the growth of whiskers. The MO_x must be present and able to be reduced to MO_{x-1} vapor. If the sub-oxides MO_{x-1} vapor were not generated during the reactions at the fabrication temperature, no Al_2O_3 whisker growth will occur. The MoO_2, WO_2, and SiO are the possible intermediate vapor products

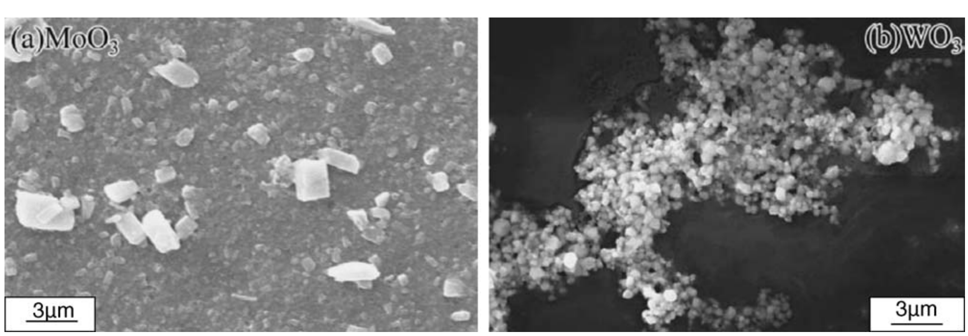

Fig. 4. SEM micrographs show (a) MoO_3 powder (in white), and (b) WO_3 powder (in white).

in the reactions during sintering of the Al–MoO_3, Al–WO_3 and Al–SiO_2, respectively. As for the other Al–MO_x systems such as Al–NiO, Al–ZnO and Al–CuO, the sub-oxide does not exist for the first two systems, while Cu_2O does not exist in vapor form at such fabricating temperature. The fact that no whisker is observed in the sintered products of Al–NiO, Al–ZnO and Al–CuO consolidates our claim that sub-oxide MO_{x-1} is the necessary intermediate product for the growth of whiskers.

5. Conclusions

We have made use of a low-cost powder metallurgy method to fabricate single-crystal α-Al_2O_3 whiskers and nanorods. The process involves the sintering of Al–MO_x powder (MO_x = MoO_3, WO_3, and SiO_2) at relatively low temperature. The Ostwald ripening mechanism is used to describe the growth of whiskers in these systems. We conclude that MO_x is necessary to provide oxygen to oxidize Al. The growth of Al_2O_3 whiskers involves the presence of MO_{x-1} and Al_2O vapors, and the size of whiskers depends on the size of the starting MO_x powder.

Acknowledgements

This work was partially funded by The Chinese University of Hong Kong—United College Lee Hysan Foundation and Endowment Fund Research Grant Scheme (Project code: CA11059), and supported by the Wuhan Chenguang Project Fund (Project code: 20035002016-14).

References

1. Zhao, Q., Zhai, G. J., Ng, D. H. L., Zhang, X. Z. and Chen, Z. Q., Surface modifications of Al_2O_3 bioceramic by NH_2^+ ion implantation. *Biomaterials*, 1999, **20**, 595–599.
2. Jankowiak, R., Roberts, K., Tomasik, P., Sikora, M., Small, G. J. and Schilling, C. H., Probing the crystalline environment of α-alumina via luminescence of metal ion impurities: an optical method of ceramic flaw detection. *Mater. Sci. Eng. A*, 2000, **281**, 45–55.
3. Webb, W. W. and Forgeng, W. D., Growth and defect structure of sapphire microcrystals. *J. Appl. Phys.*, 1957, **28**, 1449–1454.
4. Li, Y. F., Qin, C. D. and Ng, D. H. L., Morphology and growth mechanism of alumina whiskers in aluminum-based metal matrix composites. *J. Mater. Res.*, 1999, **14**, 2997–3000.
5. Lijima, S., Helical microtubules of graphitic carbon. *Nature*, 1991, **354**, 56–58.
6. Tang, C. C., Fan, S. S., Li, P., Lamy de la Chapelle, M. and Dang, H. Y., In situ catalytic growth of Al_2O_3 and Si nanowires. *J. Crystal Growth*, 2001, **224**, 117–121.
7. Zhou, J., Deng, S. Z., Chen, J., She, J. C. and Xu, N. S., Synthesis of crystalline alumina nanowires and nanotrees. *Chem. Phys. Lett.*, 2002, **365**, 505–508.
8. Zhang, Y. J., Liu, J., He, R. R., Zhang, Q., Zhang, X. and Zhu, J., Synthesis of alumina nanotubes using carbon nanotubes as templates. *Chem. Phys. Lett.*, 2002, **360**, 579–584.
9. Yan, L., Zhuang, J., Sun, X. M., Deng, Z. X. and Li, Y. D., Formation of rod-like $Mg(OH)_2$ nanocrystallites under hydrothermal conditions and the conversion to MgO nanorods by thermal dehydration. *Mater. Chem. Phys.*, 2002, **76**, 119–122.
10. Gao, Y. H., Bando, Y., Sato, T., Zhang, Y. F. and Gao, X. Q., Synthesis, Raman scattering and defects of β-Ga_2O_3 nanorods. *Appl. Phys. Lett.*, 2002, **81**, 2267–2269.
11. Wu, J. J. and Liu, S. C., Low-temperature growth of well-aligned ZnO nanorods by chemical vapor deposition. *Adv. Mater.*, 2002, **14**, 215–218.
12. Zheng, B., Wu, Y. Y., Yang, P. D. and Liu, J., Synthesis of ultra-long and highly oriented silicon oxide nanowires from liquid alloys. *Adv. Mater.*, 2002, **14**, 122–124.
13. Hacohen, Y. R., Popovitz-Biro, R., Grunbaum, E., Prior, Y. and Tenne, R., Vapor–liquid–solid growth of $NiCl_2$ nanotubes via reactive gas laser ablation. *Adv. Mater.*, 2002, **14**, 1075–1078.
14. Dai, H. J., Wong, E. W., Lu, Y. Z., Fan, S. S. and Lieber, C. M., Synthesis and characterization of carbide nanorods. *Nature*, 1995, **375**, 769–772.
15. Seeger, T., Kohler-Redlich, P. and Ruhle, M., Synthesis of nanometer-sized SiC whiskers in arc-discharge. *Adv. Mater.*, 2000, **12**, 279–282.
16. Yang, P. D. and Lieber, C. M., Nanorod-superconductor composites: a pathway to materials with high critical current densities. *Science*, 1996, **273**, 1836–1840.
17. Quate, C. F., Scanning probes as a lithography tool for nanostructures. *Surf. Sci.*, 1997, **386**, 259–264.
18. Alivisatos, A. P., Semiconductor clusters, nanocrystals, and quantum dots. *Science*, 1996, **271**, 933–937.
19. Yu, Z. Q., Chang, D., Li, C., Zhang, N., Feng, Y. Y. and Dai, Y. Y., Blue photoluminescent properties of pure nanostructured γ-Al_2O_3. *J. Mater. Res.*, 2001, **16**, 1890–1893.
20. Peng, X. S., Zhang, L. D., Meng, G. W., Wang, X. F., Wang, Y. W., Wang, C. Z. *et al.*, Photoluminescence and infrared properties of α-Al_2O_3 nanowires and nanobelts. *J. Phys. Chem. B*, 2002, **106**, 11163–11167.
21. Hornyak, G., Kroll, M., Pugin, R., Sawitowski, T., Schmid, G., Bovin, J. O. *et al.*, Gold cluster and colloids in alumina nanotubes. *Chem. Eur. J.*, 1997, **12**, 1951–1956.
22. Cooke, T. F., Inorganic fibers—a literature review. *J. Am. Ceram. Soc.*, 1991, **74**, 2959–2978.
23. Deng, C. J., Yu, P., Yau, M. Y., Ku, C. S. and Ng, D. H. L., Fabrication of single crystal α-Al_2O_3 nanorods by displacement reactions. *J. Am. Ceram. Soc.*, 2003, **86**, 1385–1388.
24. Wagner, R. S. and Ellis, W. C., Vapor–liquid–solid mechanism of single crystal growth. *Appl. Phys. Lett.*, 1964, **4**, 89–90.
25. Milewski, J. V., Gac, F. D., Petrovic, J. J. and Skaggs, S. R., Growth of beta-silicon carbide whiskers by the VLS process. *J. Mater. Sci.*, 1985, **20**, 1160–1166.
26. Chen, N. W., Readey, D. W. and Moore, J. J., Mechanisms of oxide whiskers growth. *Ceram. Eng. Sci. Proc.*, 1994, **77**, 170–180.
27. Kim, C. and Somorjai, G. A., Preparation and reaction studies of Pt/Al_2O_3 model catalysts. *J. Kor. Vac. Soc.*, 1995, **3**, 414–419.
28. Valcarcel, V., Souto, A. and Guitian, F., Development of single-crystal α-Al_2O_3 fibers by vapor–liquid–solid deposition (VSL) from aluminum and powdered silica. *Adv. Mater.*, 1998, **10**, 138–140.
29. Voorhees, P. W., Ostwald ripening of two-phase mixtures. *Annu. Rev. Mater. Sci.*, 1992, **22**, 197–215.
30. Wang, W. Z., Xu, C. K., Wang, G. H., Liu, Y. K. and Zheng, C. L., Preparation of smooth single-crystal Mn_3O_4 nanowires. *Adv. Mater.*, 2002, **14**, 837–840.
31. Brewer, L. and Searcy, A., The gaseous species of the Al–Al_2O_3 system. *J. Am. Chem. Soc.*, 1951, **73**, 5308–5314.
32. Sosman, R. B., New and old phases of silica. *Trans. Br. Ceram. Soc.*, 1955, **54**, 655–670.
33. Chiang, Y. M., Birnie, D. and Kingery, W. D., *Physical Ceramics*. John Wiley and Sons, New York, 1997, p. 359.